J. Marine Sci. Appl. (2013) 12: 406-412
DOI: 10.1007/s11804-013-1211-0

Hydrodynamic Performance Analysis of Propeller-rudder System with the Rudder Parameters Changing

Lixun Hou*, Chao Wang, Xin Chang, and Sheng Huang

College of Shipbuilding Engineering, Harbin Engineering University, Harbin 150001, China

Abstract: In order to study the effects of geometric parameters of the rudder on the hydrodynamic performance of the propeller-rudder system, the surface panel method is used to build the numerical model of the steady interaction between the propeller and rudder to analyze the relevant factors. The interaction between the propeller and rudder is considered through the induced velocities, which are circumferentially averaged, so the unsteady problem is translated to steady state. An iterative calculation method is used until the hydrodynamic performance converges. Firstly, the hydrodynamic performance of the chosen propeller-rudder system is calculated, and the comparison between the calculated results and the experimental data indicates that the calculation program is reliable. Then, the variable parameters of rudder are investigated, and the calculation results show that the propeller-rudder spacing has a negative relationship with the efficiency of the propeller-rudder system, and the rudder span has an optimal match range with the propeller diameter. Futhermore, the rudder chord and thickness both have a positive correlation with the hydrodynamic performance of the propeller-rudder system.
Keywords: rudder geometric parameters; propeller-rudder system; induced velocity; surface panel method; efficiency; hydrodynamic performance

Article ID: 1671-9433(2013)04-0406-07

1 Introduction

As the world's energy shortage gets increasingly more serious and the ship energy efficiency design index (EEDI) came into effect on January 1, reducing fuel consumption is not just about the operating costs but new considerations have to be accounted for, namely ships cannot dock in ports without meeting certain requirements and restrictions which must meet the high demands of the EEDI, affecting the normal operations and resulting in more serious economic losses.

The propeller-rudder assembly system is a kind of ship propulsion plant, through designing the rudder structure reasonably to optimize the hydrodynamic interference between the propeller and the rudder, the purpose of energy savings can be realized. Therefore, it is a topic worthy of discussion to raise the propulsion efficiency and to achieve the purpose of energy savings by improving the cooperation between the propeller and the rudder. Consulting the current literature about propeller-rudder interference, it has been found that the related research has been lacking, and most of the research focuses on the theoretical predictions for the given propeller-rudder system (Jiang, 1993; Guo, 2006; Hassan, 2008; Ma and Qian, 2005; Isay, 1965; Felli, 2011), Sun *et al*. (2012) studied the effects of the distance between the propeller and the rudder on the propeller propulsive performance through theoretical prediction combined tests, but the effects of the rudder geometric parameters on the propeller-rudder system was not studied.

This paper establishes a numerical calculation model for the steady hydrodynamic performance of the propeller-rudder system based on the surface panel method theory, and studies the effects of the parameter changes of the rudder on the hydrodynamic performance of the propeller- rudder system systematically.

2 Numerical calculation model

2.1 Surface panel method theory based on lifting body

Based on the third Green's theorem (Su, 1999; Palk, 2010; Su and Liu, 2012), considering that the body works in the irrotational, inviscid and incompressible flow with the speed of V_0, the perturbation potential of any field point $P(x,y,z)$ can be defined as follows:

$$4\pi E\phi(P)=\iint_{S_b+S_\infty}\left[\phi(Q)\frac{\partial}{\partial n_Q}(\frac{1}{R_{PQ}})-\frac{\partial\phi(Q)}{\partial n_Q}\frac{1}{R_{PQ}}\right]\mathrm{d}S \quad (1)$$

where S_b represents the body surface and its trailing vortex sheet; S_∞ represents the outside interface, when the distance between the outside control surface and the lifting body is infinite, $\nabla\varphi\to 0$; R_{PQ} is the distance from the field point P to another point Q; $\partial\varphi(Q)/\partial n_Q$ is the normal derivative of the velocity potential of the point Q on the body, and meets the impenetrable condition at the surface; E is the Green's theorem parameters, its value is defined according to the relationship between point P and the body surface S. E is zero when P within S; E is 0.5 when P is on S; E is 1.0 when

Received date: 2013-05-21.
Accepted date: 2013-09-12.
Foundation item: Supported by the China Postdoctoral Science Foundation (Grant No.2012M512133), the National Natural Science Foundation of China (Grant NO.41176074) and the Fundamental Research Funds for the Central University (Grant No.T013513015).
***Corresponding author Email:** 07093129@163.com

P is outside S.

On each part of the interface, the following boundary conditions should be met too.

$$\nabla\varphi \to 0 \quad (\text{on } S_B) \tag{2}$$

$$\partial\varphi/\partial n_Q = -\mathbf{V}_0 \cdot \boldsymbol{n}_Q \quad (S_\infty \to \infty) \tag{3}$$

$$\begin{aligned} &p^+ - p^- = 0 \\ &(\partial\varphi/\partial n_{Q_1})^+ - (\partial\varphi/\partial n_{Q_1})^- = 0 \end{aligned} \quad (\text{on } S_W) \tag{4}$$

where V_0 represents the inflow velocity, Q_1 is the point on the wake surface and superiors + and – are used respectively to mark the values of the upper and lower sides of the body.

Considering about the above three conditions, on the boundary surface the integral equation (1) can be written as

$$\begin{aligned} 2\pi\varphi(P) = &\iint_{S_B} \varphi(Q)\frac{\partial}{\partial n_Q}(\frac{1}{R_{PQ}})\mathrm{d}S + \iint_{S_W} \Delta\varphi(Q_1)\frac{\partial}{\partial n_{Q1}}(\frac{1}{R_{PQ_1}})\mathrm{d}S + \\ &\iint_{S_B} (\mathbf{V}_0 \cdot \mathbf{n}_Q)(1/R_{PQ})\mathrm{d}S \qquad (\text{on } S_B) \end{aligned} \tag{5}$$

where $\Delta\varphi$ is the potential jump across the wake surface which can be expressed by the following equation

$$\Delta\varphi = \varphi^+ - \varphi^-$$

The potential jump $\Delta\varphi$ across the wake surface is determined through the pressure Kutta condition, which requires that the pressure difference between the two sides of the lifting body at the trailing edge is zero, that is

$$(\Delta p)_{TE} = p_{TE}^+ - p_{TE}^- = 0 \tag{6}$$

Employing the pressure Kutta condition, the integral equation (5) can be uniquely solved by means of numerical iterative method.

2.2 Solving method of propeller-rudder interference

The interference between the propeller and the rudder is considered through induced velocities during calculation (Su *et al.*, 1999; Tomasz, 2010; Qin, 2008). According to the integral equation (5), the velocity potential on the propeller and the rudder can be defined as follows:

$$\begin{aligned} 2\pi\phi(P) = &\iint_{S_P} \phi(Q)\frac{\partial}{\partial n_Q}\frac{1}{R_{PQ}}\mathrm{d}S + \iint_{S_{PW}} \Delta\phi(Q_1)\frac{\partial}{\partial n_Q}\frac{1}{R_{PQ_1}}\mathrm{d}S + \\ &\iint_{S_P} [(V_0 + r\boldsymbol{\Omega}_\theta + V_{pd}) \cdot n_Q]\frac{1}{R_{PQ}}\mathrm{d}S \end{aligned} \tag{7}$$

$$\begin{aligned} 2\pi\phi(P) = &\iint_{S_d} \phi(Q)\frac{\partial}{\partial n_Q}\frac{1}{R_{PQ}}\mathrm{d}S + \iint_{S_{dW}} \Delta\phi(Q_1)\frac{\partial}{\partial n_Q}\frac{1}{R_{PQ_1}}\mathrm{d}S + \\ &\iint_{S_d} [(V_0 + V_{dp}) \cdot n_Q]\frac{1}{R_{PQ}}\mathrm{d}S \end{aligned} \tag{8}$$

where S_p, S_{pw}, S_d, S_{dw} represent propeller surface, propeller wake surface, rudder surface and rudder wake surface respectively; Ω_θ is the rotational speed of the propeller; V_{pd}, V_{dp} represent the induced velocities the rudder has on the surface of the propeller and those the propeller has on the surface of the rudder; n_Q is the unit normal vector on the boundary surface and points to the flow field inside.

The surfaces of the propeller, the rudder and their wake are divided into panels, as shown in Fig. 1. The cosine spacing is employed in the chord wise direction and span wise direction of both the propeller blade and the rudder. What's more, the trailing vortex model is linear.

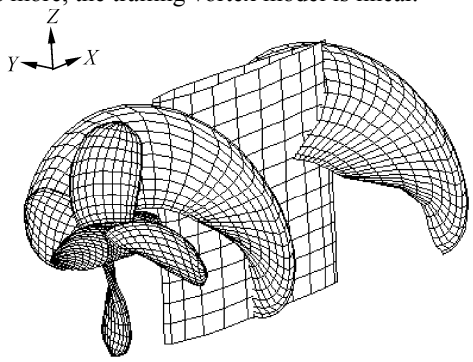

Fig.1 Calculation model of propeller and rudder

The integral equations (7) and (8) can be discretized as

$$\sum_{j=1}^{N_p}(\delta_{ij} - C_{ij})\phi_j^k - \sum_{m=1}^{N_{pw}} W_{im}\Delta\phi_m^k = -\sum_{j=1}^{N_p} B_{ij}\{[V_0 + r\boldsymbol{\Omega}_\theta + (V_{pd}^k)_j] \cdot n_j\}$$

i=1,2,…, N_p （9）

$$\sum_{j=1}^{N_d}(\delta_{ij} - C_{ij})\phi_j^k - \sum_{l=1}^{N_{dw}} W_{il}\Delta\phi_l^k = -\sum_{j=1}^{N_d} B_{ij}\{[V_0 + (V_{dp}^k)_j] \cdot n_j\}$$

i=1,2,…,N_d （10）

where subscripts p and d represent the propeller and the rudder; dp and pd represent the effect of the propeller on the rudder and the effect of the rudder on the propeller respectively; V_{pd}^k, V_{dp}^k represent the induced velocities that the rudder has on the surface of the propeller and the induced velocities that the propeller has on the surface of the rudder at K iteration. $V_{pd}^0 = 0$、$V_{dp}^0 = 0$ represents that the propeller is in open water conditions and the induced velocity that the propeller in open water has on the surface of the rudder. Getting the gradient of the integral equations (7) and (8), the following equations can be gotten:

$$\begin{aligned} V_{dp}^k = &\sum_{j=1}^{N_p}\phi_J^k\nabla C_{ij} + \sum_{l=1}^{N_{pw}}\Delta\phi_l^k\nabla W_{il} + \\ &\sum_{j=1}^{N_p}\{[V_0 + r\boldsymbol{\Omega}_\theta + (V_{pd}^{k-1})_j] \cdot n_j\}\nabla B_{ij} \end{aligned} \quad i=1, 2,\ldots, N_p \tag{11}$$

$$\begin{aligned} V_{pd}^k = &\sum_{j=1}^{N_p}\phi_J^k\nabla C_{ij} + \sum_{m=1}^{N_{dw}}\Delta\phi_m^k\nabla W_{im} + \\ &\sum_{j=1}^{Nd}\{[V_0 + (V_{dp}^{k-1})_j] \cdot n_j\}\nabla B_{ij} \end{aligned} \quad i=1,\ 2,\ldots,\ N_d \tag{12}$$

where ∇C , ∇W , ∇B are velocity influence coefficients, which can be calculated using Morino's analytical formulation.

According to the integral equations (11) and (12), combining the pressure Kutta condition of the propeller and the rudder, V_{dp}^k and V_{pd}^k can be calculated. Then, the discretized equations (9) and (10) can be solved and the velocity distribution of the propeller and the rudder can be determined. According to the Bernoulli's integral equation, the pressure distribution on the surface of the body can be determined. The hydrodynamic performance of the propeller-rudder system can be defined as:

$$K_{TP}=\frac{T_p}{\rho n^2 D^4};K_Q=\frac{Q_p}{\rho n^2 D^5};\eta_P=\frac{K_{TP}}{K_Q}\frac{J}{2\pi}$$

$$K_{Td}=\frac{T_d}{\rho n^2 D^4};K_{TZ}=K_{TP}+K_{Td};\eta_Z=\frac{K_{TZ}}{K_Q}\frac{J}{2\pi}$$

where, K_{TP}, K_Q represent the propeller's thrust coefficient and torque coefficient; K_{Td} represents the rudder's thrust coefficient; K_{TZ}, η_Z represent the thrust coefficient and propulsive efficiency of the propeller-rudder system; T_p and T_d represent the propeller's thrust and the rudder's thrust; Q_p represents the propeller's torque; η_P represents the propeller's efficiency; J represents the advance coefficient; ρ represents the fluid density; D represents the propeller's diameter; n represents the propeller's rotational speed.

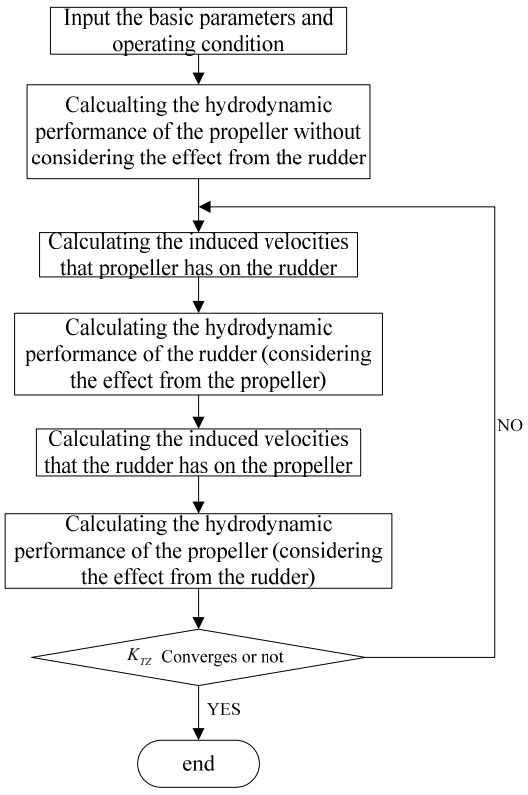

Fig.2 Flowchart of interaction calculation

2.3 Iterative process

Firstly, the open water hydrodynamic performance of the propeller is calculated. Then, regarding the induced velocities that the propeller has on the rudder as a part of the inflow of the rudder the hydrodynamic performance of the rudder is calculated. Next, the hydrodynamic performance of the propeller with consideration for the interference from the rudder is calculated. An iterative process is adopted until K_{TZ} converges. The design process is shown in Fig.2.

3 Calculation results and analysis

Table1 and Table2 give the parameters of the calculation model used in this paper (Wang and Zhang, 1987; PEI and YANG, 1994). The method given above is used to calculate the propeller-rudder system. The panel dividing method, panel number and the trailing vortex model of the propeller and the rudder are kept unchanged, and the rudder angle is always zero. In order to analyze the effects of rudder parameters on the hydrodynamic performance of the propeller-rudder system, this paper has mutative scale calculations of the propeller-rudder spacing, the rudder span, rudder chord length and thickness respectively.

Table 1 Geometric parameters of propeller

pattern	A/A_0	P/D	D/m
B4-55	0.55	1.0	0.24

Table 2 Geometric parameters of rudder

Section pattern	Aspect ratio	Rudder span(m)
NACA0020	1.0	0.24

3.1 Model reliability analysis

As (Wang and Zhang, 1987) just gives the propeller's efficiency experimental results of the propeller-rudder system, so this section validates the calculation program by comparing the calculated value with the experimental results of the propeller.

The distance between the propeller and the rudder is 0.516D. As shown in Fig.3, the calculated values are consistent with the experimental results of the forward propeller's efficiency. The difference is greater at low or high advance coefficients. This is mainly because this calculation program is based on potential flow theory ignoring the viscosity influence, and results in the larger differences at low advance coefficients. On the other hand, the trailing vortex has obvious deformation at high advance coefficients actually. However, the trailing vortex model adopted in this paper is linear, so the effect of the trailing vortex is the main reason for differences at high advance coefficients.

As the maximum value that the calculated data deviates from the experimental results is 3.2%, so the calculation program is thought to have good accuracy, and the result of the calculation is reliable. Therefore, the next calculation can be carried out.

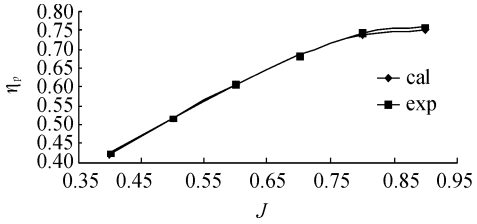

Fig. 3 Comparison of propeller performance between calculation and experimental data

3.2 The effect of the propeller-rudder spacing on the hydrodynamic performance of the propeller-rudder system

In order to analyze the effect of the spacing between the forward propeller and the after rudder on the propeller-rudder system, the efficiency of the propeller-rudder system is calculated, with the ratio of the spacing (*d*) and the propeller diameter (*D*) adopting 0.3, 0.35, 0.4, 0.45, 0.5, 0.55, 0.6, 0.65, 0.7 at the advance coefficient of 0.7 respectively.

Fig.4 shows the propeller-rudder system and the propeller efficiency's changing trend along with the spacing between the forward propeller and the after rudder. As shown in the chart, the efficiency of the propeller-rudder system has an evident increment comparing with the propeller, and the efficiencies of the propeller-rudder system and the propeller both decrease with the increasing of the propeller-rudder spacing significantly. The conclusion is consistent with the literature (Sun, 2012). Therefore, the spacing between the propeller and the rudder ought to adopt as little value as possible with the conditions permitting. In the following study, the propeller-rudder spacing always adopts 0.516*D*.

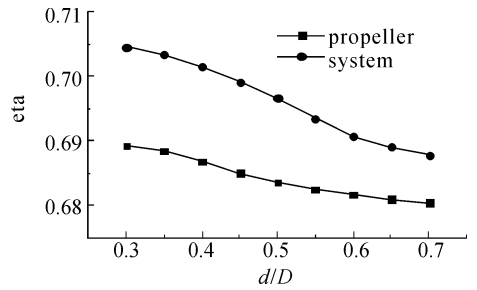

Fig.4 Efficiency at different propeller-rudder spacing

3.3 The effect of the rudder span on the hydrodynamic performance of the propeller-rudder system

In order to analyze the effect of the rudder span on the propeller-rudder system, the efficiency of the propeller-rudder system is calculated with the ratio of the rudder span (*B*) and the propeller diameter (*D*) adopting 0.5, 0.7, 0.9, 1.1, 1.3, 1.5, 1.7, 1.9 at advance coefficients of 0.5, 0.7, 0.9, 1.1 respectively.

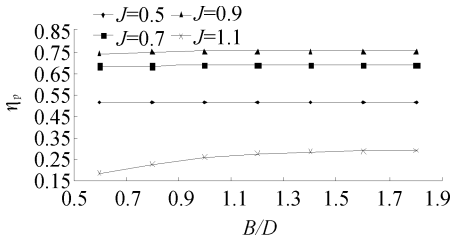

Fig.5 Propeller efficiency at different rudder spans

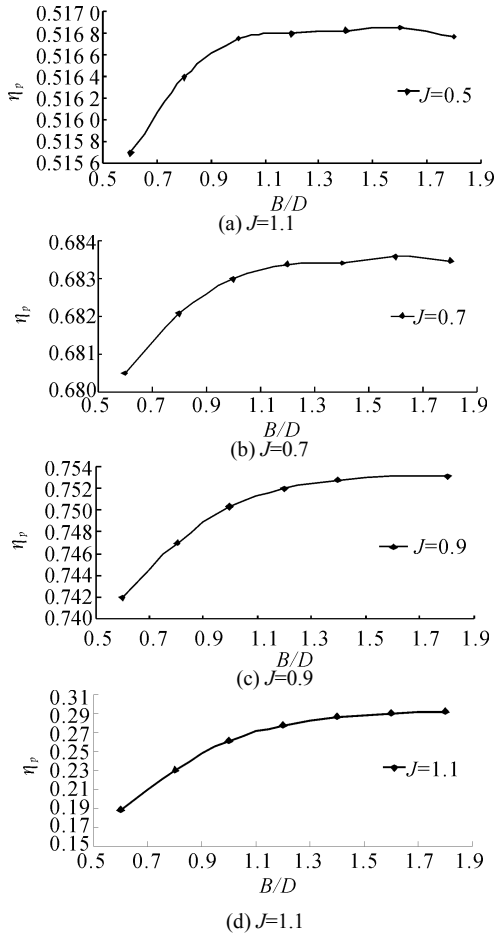

Fig.6 Propeller efficiency at different rudder spans and advance coefficients

Fig. 5 shows the effect of the rudder span on the propeller efficiency η_P at different advance coefficients. As shown in the chart, the propeller efficiency η_P changes significantly with the rudder span and has an increasing trend at higher advance coefficients. However, the changing trend is not obvious at lower advance coefficients. Fig.6 can be obtained after partially enlarged. As shown in Fig.6, the propeller efficiency increases significantly along with the increasing of the rudder span when the rudder span is smaller. The propeller efficiency starts to level off and the added value is smaller when the rudder span reaches 1.2 times the propeller diameter. However, the propeller efficiency has a decreasing trend when the rudder span is greater than 1.6 times the propeller diameter.

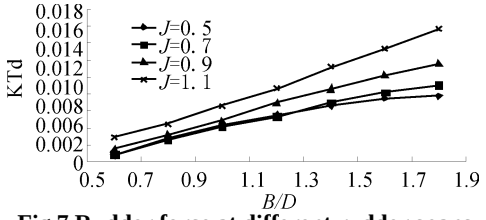

Fig.7 Rudder force at different rudder spans

Fig. 7 shows the changing trend of the rudder thrust coefficient K_{Td} along with the rudder span. As shown in the chart, K_{Td} is larger with higher advance coefficients, and is positively related to the rudder span. That is, the rudder's contribution to the thrust of the propeller-rudder system is greater with the rudder span being longer at higher advance coefficients.

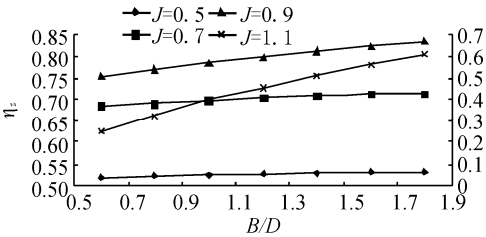

Fig.8 propeller-rudder efficiency at different rudder spans

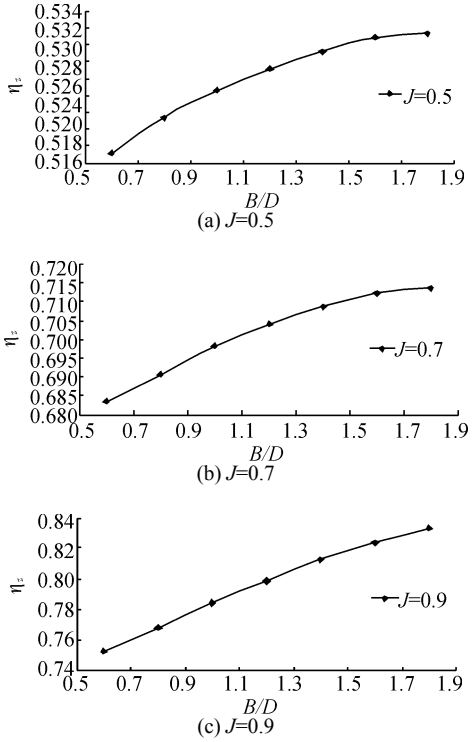

Fig.9 Propeller-rudder efficiency at different rudder spans and advance coefficients

Fig.8 shows the changing trend of the propeller-rudder system efficiency η_Z along with the rudder span at difference advance coefficients. The double coordinate system is adopted, J=1.1 corresponds to the right side of the coordinate. As shown in Fig.8, η_Z changes significantly along with the rudder span and has an increasing trend. However, the changing trend is not obvious at low advance coefficients. After amplifying Fig.8 locally, Fig.9 is obtained. As shown in figure (a) and figure (b), the efficiency of the propeller-rudder system increases significantly when the rudder span is less than 1.5 times the propeller diameter, and starts to level off when the rudder span reaches 1.5 times the propeller diameter. When J is greater than 0.9, the efficiency has a strictly increasing trend along with the increasing of the rudder span.

From the above analysis, the propeller efficiency has already reached a stable state when the rudder span has reached 1.2 times the propeller diameter. With J less than 0.9, on the other hand, the propeller-rudder system starts to level off when the rudder span reaches 1.5 times the propeller diameter owing to the rudder's contribution to the thrust of the propeller-rudder system. The efficiency of the propeller-rudder system has a strictly increasing trend along with the increasing of the rudder span. For the propeller-rudder system adopted in this paper, the perfect rudder span interval is 1.2–1.5 times the propeller diameter at low advance coefficients. Because in this range the propeller has already reached optimal performance, and the performance of the propeller-rudder system remains stable. At high advance coefficients, the rudder span should be as long as possible. However, the specific rudder span should be taken with a comprehensive consideration of the stern space and economics.

3.4 The effects of the rudder chord length on the hydrodynamic performance of the propeller-rudder system

In order to analyze the effects of the rudder chord length on the hydrodynamic performance of the propeller-rudder system, the rudder span adopts 1.2 times the propeller diameter and the ratio of the rudder chord length (C) and the rudder span (B) adopts 0.4, 0.6, 0.8, 1.0, 1.2, 1.4 respectively, the reciprocal of which is the aspect ratio. The efficiency of the propeller-rudder system is calculated at advance coefficients of 0.5, 0.7, 0.9, 1.0, 1.1, respectively.

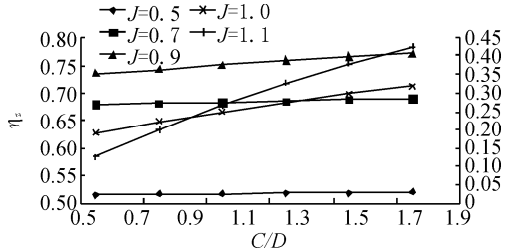

Fig.10 propeller-rudder efficiency at different chord lengths of the rudder

Fig. 10 shows the effects of the rudder chord length on the propeller-rudder system efficiency, the double coordinate system is adopted, J=1.1 corresponds to the right side of the coordinates. As shown in Fig.10, the efficiency increases significantly along with the increasing of the rudder chord

length at high advance coefficients of 0.9, 1.0, 1.1. However, the efficiency is relatively stable at low advance coefficients of 0.5, 0.7.

From the above analysis, high aspect ratio rudders should be adopted considering the manufacturing cost and steerability at low advance coefficients. However, the rudders chosen should be as low aspect ratio as possible for the purpose of meeting economy at high advance coefficients.

3.5 The effects of the rudder thickness on the hydrodynamic performance of the propeller-rudder system

In order to analyze the effects of the rudder thickness on the hydrodynamic performance of the propeller-rudder system, the rudder span adopts 1.2 times the propeller diameter, and the rudder chord length (*C*) is 0.8 times the rudder span, in other words, the aspect ratio is 1.25. The rudder section adopts NACA0010, NACA0012, NACA0015, NACA0018, NACA0021 and NACAOO24 which are mature symmetric airfoils and stands for six different thickness distributions. The efficiency of the propeller-rudder system is calculated at advance coefficients of 0.5, 0.7, 0.9, 1.0, 1.1 respectively.

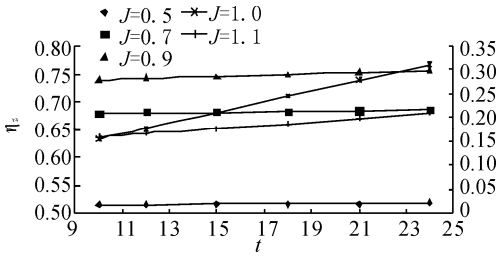

Fig.11 propeller efficiency at different rudder thickness

As shown in Fig.11, *t* represents the ratio of the rudder section maximum thickness and the chord length multiplying by 100, for example, *t*=15 means that the airfoil is NACA0015 and that the ratio of the maximum thickness and the chord length is 15%. *J*=1.1 corresponds to the right side of the coordinates. As shown in the chart, the effects of rudder thickness on the propeller-rudder system is consistent with the chord length, the efficiency increases significantly along with the increasing of the rudder chord length at high advance coefficients of 1.0, 1.1. However, the efficiency is relatively stable at low advance coefficients of 0.5, 0.7, 0.9. From the above analysis, at low advance coefficients, the efficiency of the propeller-rudder system keeps unchanged essentially along with the increasing of the rudder thickness. Therefore, considering the cost problem, the rudder thickness ought to adopt as little value as possible on the premise that the strength requirement has been satisfied. On the other hand, the rudder thickness should take as large a value as possible on the condition that the economics is satisfied at high advance coefficients.

4 Conclusion

Based on the potential flow theory, this paper calculates the effects of the rudder parameters including the propeller-rudder spacing, the rudder span, chord length and thickness on the hydrodynamic performance of the propeller-rudder system. Through analyzing the calculation results, the following conclusions have been obtained:

1) The effects of the spacing of the forward propeller and the after propeller on the hydrodynamic performance of the propeller-rudder system is evident, the efficiency of the system has an evidently incremental comparison with the propeller, and the efficiencies of the propeller-rudder system and the propeller both decrease with the increasing of the propeller-rudder spacing significantly.

2) The rudder span has an effect on the hydrodynamic performance of the propeller-rudder system, and it's more significant at high advance coefficients. When the propeller diameter is given, the rudder span has an optimal range. For the propeller-rudder system used in this paper, the optimal range of the rudder span is 1.2–1.5 times the propeller diameter when the advance coefficient is less than 0.9. Otherwise, the rudder span ought to adopt as large a value as possible.

3) The effects of the rudder chord length on the hydrodynamic performance of the propeller-rudder system is consistent with the rudder thickness. For the propeller-rudder system used in this paper, the effect of the chord length and thickness on the performance of the propeller-rudder system remains about the same. However, when the advance coefficient is larger than 0.9, the efficiency of the system increases significantly along with the increasing of the rudder chord length and thickness.

The trailing vortex of the propeller has deformation during rotation and has significant effect on the performance of the propeller. However, the trailing vortex model used in this paper is linear. Although the accuracy requirements are satisfied, there is room yet to be improved. On the other hand, the analysis this paper has in regards to the interference between the propeller and the rudder was developed under the condition that the rudder angle is zero. Therefore, studying the hydrodynamic performance of the propeller-rudder system under different rudder angles and the trailing vortex nonlinear study will be the next research topics.

References

Felli M (2011). Propeller tip and hub vortex dynamics in the interaction with a rudder. *Experiments in Fluids,* **51**(5), 1385-1402.

Guo Chunyu (2006). Numerical calculation of the hydrodynamic performance of the propeller-rudder additional thrust fin system. Ph. D thesis, Harbin Engineering University, Harbin, 57-61. (in Chinese)

Hassan G (2008). Computational hydrodynamic analysis of the propeller-rudder and the AZIPOD system. *Ocean Engineering*, **35**(1), 123-125.

Isay W (1965). On the interaction between ship and screw propeller. *Schiffstechnik*, **12**(1), 65-76.

Jiang Shaojian (1993). Hydrodynamic performance study of the propeller-rudder interference. Ph.D thesis, Shanghai Jiao Tong University, Shanghai, 60-96. (in Chinese)

Ma Cheng, Qian Zhengfang (2005). Hydrodynamic performance calculation and simulation study of the propeller-rudder-rudder ball propulsive system. *Journal of Ship Mechanics*, **9**(5), 42-43. (in Chinese)

Palk B, Kim K (2010). Influence of the propeller wake sheet on rudder gap flow and gap cavitation. *Ocean Engineering*, **37**(16),1418-1427.

Pei Weimin, Yang Huaishu (1994). The effect of the rudder ball on the hydrodynamic performance of the propeller. *Journal of Shanghai Shipping Science Institute*, **17**(1), 9-10.

Qin Xinchuan, Huang Sheng, Chang Xin (2008). Research on the hydrodynamic interference of the four propellers and double rudders system. *Shipbuilding of China*, **49**(1), 112-116.

Sun Haisu, Su Jia, Wei Jinfang (2012). Study about the effect of propeller-rudder distance on the propulsive performance of the propeller. *Shipbuilding of China*, **52**(1), 4-6.

Su Yumin (1999). A study on design of marine propellers by lifting body theory. Ph.D thesis, Yokohama National University, Yokohama, 20-56.

Su Yumin, Liu Yebao (2012). Surface panel method- based numerical calculation for predicting ducted propeller performances. *Journal of Huazhong University of Science and Technology*, **44**(8), 58-59.

Tomasz A, Jakub H (2010). Numerical analysis of influence of the streamline rudder on the screw propeller efficiency. *Polish Maritime Research*, **17**(2), 18-22.

Wang Dexun, Zhang Zhijun (1987). Propeller-rudder interference trial study. *Journal of Wuhan Institute of Water Transportation Engineering*, **1**(11), 45-48.

Author biographies

Sheng Huang was born in 1945. He is a professor at Harbin Engineering University. His current research interests include shipbuilding engineering, marine propulsor and energy-saving.